





Article

Far-Field DOA Estimation of Uncorrelated RADAR Signals through Coprime Arrays in Low SNR Regime by Implementing Cuckoo Search Algorithm

Khurram Hameed ¹, Wasim Khan ¹, Yasser S. Abdalla ², Fatemah F. Al-Harbi ³, Ammar Armghan ^{4,*} , Muhammad Asif ^{5,*}, Muhammad Salman Qamar ^{1,6}, Farman Ali ^{6,*}, Md Sipon Miah ⁷ , Mohammad Alibakhshikenari ^{7,*}  and Mariana Dalarsson ^{8,*} 

- ¹ Department of Electrical Engineering, International Islamic University, Islamabad 44000, Pakistan; khurram.phdee112@iiu.edu.pk (K.H.); wasim.khan@iiu.edu.pk (W.K.); mskhan131@qurtuba.edu.pk (M.S.Q.)
- ² Department of Computer Engineering and Networks, College of Computer and Information Sciences, Jouf University, Sakaka 72388, Saudi Arabia; ysabdalla@ju.edu.sa
- ³ Department of Physics, College of Science, Princess Nourah Bint Abdulrahman University, P.O. Box 84428, Riyadh 11671, Saudi Arabia; ffalharbi@pnu.edu.sa
- ⁴ Department of Electrical Engineering, College of Engineering, Jouf University, Sakaka 72388, Saudi Arabia
- ⁵ Department of Electrical Engineering, University of Science & Technology, Main Campus, Township Bannu, Bannu 28100, Pakistan
- ⁶ Department of Electrical Engineering, Qurtuba University of Science and IT, Dera Ismail Khan 29050, Pakistan
- ⁷ Department of Signal Theory and Communications, Universidad Carlos III de Madrid, Leganés, 28911 Madrid, Spain; mmiah@ing.uc3m.es
- ⁸ School of Electrical Engineering and Computer Science, KTH Royal Institute of Technology, 100-44 Stockholm, Sweden
- * Correspondence: aarmghan@ju.edu.sa (A.A.); masifeed@ustb.edu.pk (M.A.); drfarmanali.optics@qurtuba.edu.pk (F.A.); mohammad.alibakhshikenari@uc3m.es (M.A.); mardal@kth.se (M.D.)

Citation: Hameed, K.; Khan, W.; Abdalla, Y.S.; Al-Harbi, F.F.; Armghan, A.; Asif, M.; Salman Qamar, M.; Ali, F.; Miah, M.S.; Alibakhshikenari, M.; et al. Far-Field DOA Estimation of Uncorrelated RADAR Signals through Coprime Arrays in Low SNR Regime by Implementing Cuckoo Search Algorithm. *Electronics* **2022**, *11*, 558. <https://doi.org/10.3390/electronics11040558>

Academic Editor: Raed A. Abd-Alhameed

Received: 20 December 2021

Accepted: 8 February 2022

Published: 12 February 2022

Publisher's Note: MDPI stays neutral with regard to jurisdictional claims in published maps and institutional affiliations.



Copyright: © 2022 by the authors. Licensee MDPI, Basel, Switzerland. This article is an open access article distributed under the terms and conditions of the Creative Commons Attribution (CC BY) license (<https://creativecommons.org/licenses/by/4.0/>).

Abstract: For the purpose of attaining a high degree of freedom (DOF) for the direction of arrival (DOA) estimations in radar technology, coprime sensor arrays (CSAs) are evaluated in this paper. In addition, the global and local minima of extremely non-linear functions are investigated, aiming to improve DOF. The optimization features of the cuckoo search (CS) algorithm are utilized for DOA estimation of far-field sources in a low signal-to-noise ratio (SNR) environment. The analytical approach of the proposed CSAs, CS and global and local minima in terms of cumulative distribution function (CDF), fitness function and SNR for DOA accuracy are presented. The parameters like root mean square error (RMSE) for frequency distribution, RMSE variability analysis, estimation accuracy, RMSE for CDF, robustness against snapshots and noise and RMSE for Monte Carlo simulation runs are explored for proposed model performance estimation. In conclusion, the proposed DOA estimation in radar technology through CS and CSA achievements are contrasted with existing tools such as particle swarm optimization (PSO).

Keywords: cuckoo search; root mean square error; direction of arrival; root mean square error; coprime sensor arrays

1. Introduction

In radar technology, our prime concern is to detect the target through its parameters such as the direction of arrival, amplitude, frequency, velocity and scattering behaviour. In these parameters, DOA estimation is a key parameter that plays a vital role in electromagnetic spectrum sensing to locate the target. It is also applied in vast variety of applications such as sonar [1], wireless communication [2], satellite communication [3], medical applications [4], etc. In most of the literature, two famous array structures are implemented for

DOA estimation [5–7]. One of them is uniform linear arrays [8–10] and the second one is sparse arrays [11,12]. A lot of research has been done on uniform linear arrays (ULA). ULA is one of the simplest forms of antenna array structures, but it can estimate only $(N - 1)$ targets by using N antenna elements through subspace-based methods. In radar antenna array signal processing, we want to enhance freedom without increasing hardware costs. Nevertheless, sparse arrays can resolve more targets than several antenna elements. Therefore, sparse arrays have become a scorching area of research since the last decade in order to estimate DOA with an enhanced degree of freedom (DOF) precisely. In the perspective of radar technology, DOF is defined as the number of sources that can be resolved with a given number of antenna elements. Minimum redundancy array (MRA) [13,14], nested arrays (NA) [15] and coprime sensor arrays (CSA) [16] are the most prominent types of non-uniform linear arrays that provide higher degree of freedom. Moffet introduced MRA in 1968 [17] to improve the DOF, but this array structure has no closed-form expression to identify the location of antenna elements. Later on, in [18], nested array structure was proposed by PPal and PP Vaidyanathan in 2010 and this array structure is the combination of dense and sparse uniform linear sub-arrays. On the one hand, hole-free difference co-array and $O(N^2)$ DOF are the features of this array structure, but on the other hand, severe mutual coupling occurs in this array structure due to the part of dense sub-array. This mutual coupling is the primary cause of performance degradation of nested arrays in DOA estimation. Compared with these arrays structures, the coprime array structure has less mutual coupling due to its sparse array structure and higher DOF. CSA consists of two ULAs having M and N antenna elements with Nd and Md inter-element spacing, respectively, and $O(MN)$ DOF. CSA has been become more attractive for researchers due to its less mutual coupling and higher achievable DOF [19]. Therefore, this paper addressed the coprime array structure for far-field sources estimation to enhance the DOF in radar antenna array signal processing.

After receiving the signal through antenna arrays, estimation algorithms play an important role in array signal processing for parameters estimation. In most of the literature, the two most dominant algorithms are used in array signal processing for parameter estimation. One of them is deterministic algorithms, and the other is the heuristic approach. Deterministic algorithms are mostly sub-space based methods like multiple signal classification (MUSIC) [20,21], signal parameter via rotational invariance Technique (ES-PRIT) [22], root MUSIC [23], weighted subspace fitting (WSF) [24], etc. Although these algorithms perform very well in estimation accuracy, the major issue to implementing them is computational complexity. In this modern era of technology, this issue is resolved using meta-heuristic algorithms. Nobody can deny the significance of heuristic techniques such as genetic algorithm (GA) [25], particle swarm optimization (PSO) [26], differential evolution (DE) [27], simulated annealing (SA) [28], ant colony optimization (ACO) [29], bee colony optimization (BCO) [30], flower pollination algorithm (FPA) [31], cuckoo search algorithm [32] and so on. These techniques are population based, and these methods are efficient and robust. Recently in the research community, cuckoo search has become more popular due to its easy implementation and few parameters required to execute the algorithm compared with other heuristic approaches.

Following our literature review, no one has implemented the cuckoo search technique through coprime arrays for DOA estimation. Therefore, a novel approach has been executed by employing coprime antenna arrays in radar technology with an intelligent metaheuristic optimization algorithm. The structure of the paper is organized as follows. Section 2 discusses the analytical representation of the proposed CSAs, including fitness function. The presented methodology is investigated in Section 3 with the currently used PSO system. Section 4 contains the material related to results and discussion of the simulation analysis of the proposed CSA technique for DOA. The conclusion of the presented framework is summarized in Section 5.

2. Analytical Representation

2.1. Coprime Sensor Array Structure

In this part, the formation of the coprime array structure is discussed briefly, we then perform the derivation of the received signal. The coprime array comprises two coprime uniform linear arrays with P and Q antenna elements as shown in Figure 1. The inter-element distance between two consecutive antennas of the first sub-array is Qd , and in the second sub-array is Pd , which is more significant than $\lambda/2$ in both arrays. By merging these two sub-arrays, we obtain the coprime antenna array with the shared the first antenna element. P and Q are coprime integers, d is equal to the wavelength of the received signal and $P > Q$ for the sake of generality. M_P and M_Q shows the indexes of sub-array 1 and 2 while $M_{coprime}$ demonstrates the positions of the coprime array. This coprime array consists of $P + Q - 1$ antenna elements having non-uniform inter-element distance among them, as depicted in the following equations.

$$M_P = \{0, Qd, 2Qd, 3Qd, \dots, (P - 1)Qd\} \tag{1}$$

$$M_Q = \{0, Pd, 2Pd, 3Pd, \dots, (Q - 1)Pd\} \tag{2}$$

$$M_{coprime} = \{0, Qd, Pd, 2Qd, 2Pd, \dots, (Q - 1)Pd, (P - 1)Qd\} \tag{3}$$

2.2. Signal Modelling

In this module, we will establish the signal model for L narrowband uncorrelated unknown sources. Figure 1 shows each parameter of CSA for physical location and estimated as:

$$I_p = \{0, Qd, Pd, 2Qd, 2Pd, \dots, (Q - 1)Pd, (M - 1)Pd\} \tag{4}$$

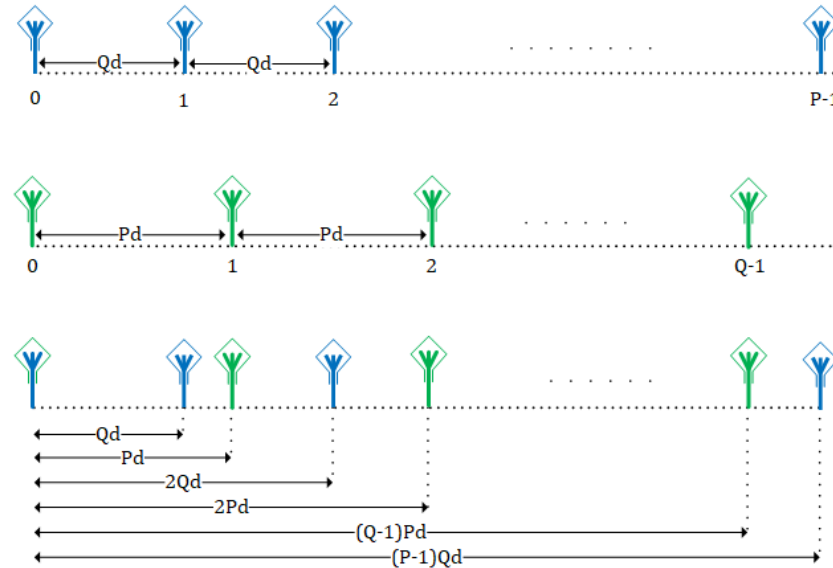


Figure 1. Generalized coprime antenna array structure.

The DOA of these L uncorrelated signals are summarized in vector Φ

$$\Phi = [\Phi_1, \Phi_2, \Phi_3, \dots, \Phi_L] \tag{5}$$

Accordingly, the received signal of L uncorrelated sources of coprime array is specified in Equation (6).

$$x(t) = \sum_{l=0}^L a_l(\Phi) s_l(t) + n(t) \tag{6}$$

where

$$a_l(\Phi) = [1, e^{\pi Q \sin \Phi_1}, e^{\pi P \sin \Phi_2}, e^{\pi 2Q \sin \Phi_3}, e^{\pi 2P \sin \Phi_4}, \dots, e^{\pi(Q-1)Pd \sin \Phi_{L-1}}, e^{\pi(P-1)Qd \sin \Phi_L}] \tag{7}$$

$$s_l(t) = [s_1(t), s_2(t), \dots, s_L(t)]^T \tag{8}$$

In Equation (6), $n(t)$ is the complex iid and AWGN with variance σI^2 and zero mean.

$$n(t) = [n_1(t), n_2(t), \dots, n_{P+Q-1}(t)] \tag{9}$$

Taking the expectation of the output signals the computation of covariance matrix can be performed in terms of coprime array framework, which are defined as

$$R_{xx} = E[x(t)x^H(t)] \tag{10}$$

where R_{xx} is the vectorization of the covariance matrix and can be further expanded as

$$R_{xx} = AR_{ss}A^H + \sigma^2 I \tag{11}$$

The covariance matrix amplitude of the output signal is denoted by R_{ss} and written as

$$R_{ss} = E[s(t)s^H(t)] \tag{12}$$

With the help of R_{xx} the virtual uniform linear array can be computed which is described as

$$z = \text{vec}(R_{xx}) = \text{vec}(AR_{ss}A^H + \sigma^2 I) = B\sigma^2 + \sigma^2 I \tag{13}$$

where B is the Kronecker product and the elements in B are expressed in the form of following equation

$$e^{jK(q_i - q_j) \sin \Phi_L}, i, j = 1, 2, \dots, P+Q-1 \tag{14}$$

In Matlab, the *vec* command is used for vectorization. After performing vectorization of R_{xx} , this matrix will become a column vector having the dimension $z^{(P+Q-1)^2 \times 1}$. Furthermore, this z vector will be sorted out in accordance with the exponent term of the received signal and presented as

$$I_c = \{(Pnd - Qmd) \cup (Qmd - Pnd)\}, \text{ where } 0 < m < P - 1 \text{ and } 0 < n < Q - 1 \tag{15}$$

The locations of these virtual ULA elements are presented as

$$I_v = \{(q_i - q_j) \mid i, j = 1, 2, \dots, P + Q - 1\} \tag{16}$$

Our prime concern is the continuous part of vULA of CSA in this research work. The continuous part of vULA causes an enhancement in the degree of freedom. Moreover, this DOF is directly proportional to the length of continuous vULA.

2.3. Fitness Function

In heuristically optimization algorithms, the fitness function plays a vital role. A fitness function is a fundamental tool for evaluating the population and provides the difference between actual and estimated angles. Based on this difference, algorithms perform their estimation, and the equation for the fitness function is written in Equation (17).

$$f(x_i) = |x_a(\Phi_i) - x_e(\Phi_i)|^2 \tag{17}$$

The nests and particles are analyzed for the fitness function's proposed setup.

3. Proposed Methodology

3.1. Cuckoo Search Algorithm

This algorithm is developed in combination with levy flights. Due to obtained accurate optimal solution, the performance of cuckoo search is much better than other meta-heuristic approaches. The direction of arrival estimation is the unconstrained optimization problem, and it is minimized by implementing a cuckoo search algorithm through the following function

$$\text{Minimize } f(\Phi) = |\Phi_a - \Phi_e|^2; \text{ where } 0 \leq \Phi_a, \Phi_e \leq \pi \quad (18)$$

$f(\Phi)$ is the fitness function and is also known as the objective function while Φ_a and Φ_e are actual and estimated angles respectively and these are optimized by evaluating the objective function through the cuckoo search algorithm. The evolution process of the cuckoo search algorithm is elaborated in Algorithm 1, and the flow diagram of cuckoo search is depicted in Figure 2.

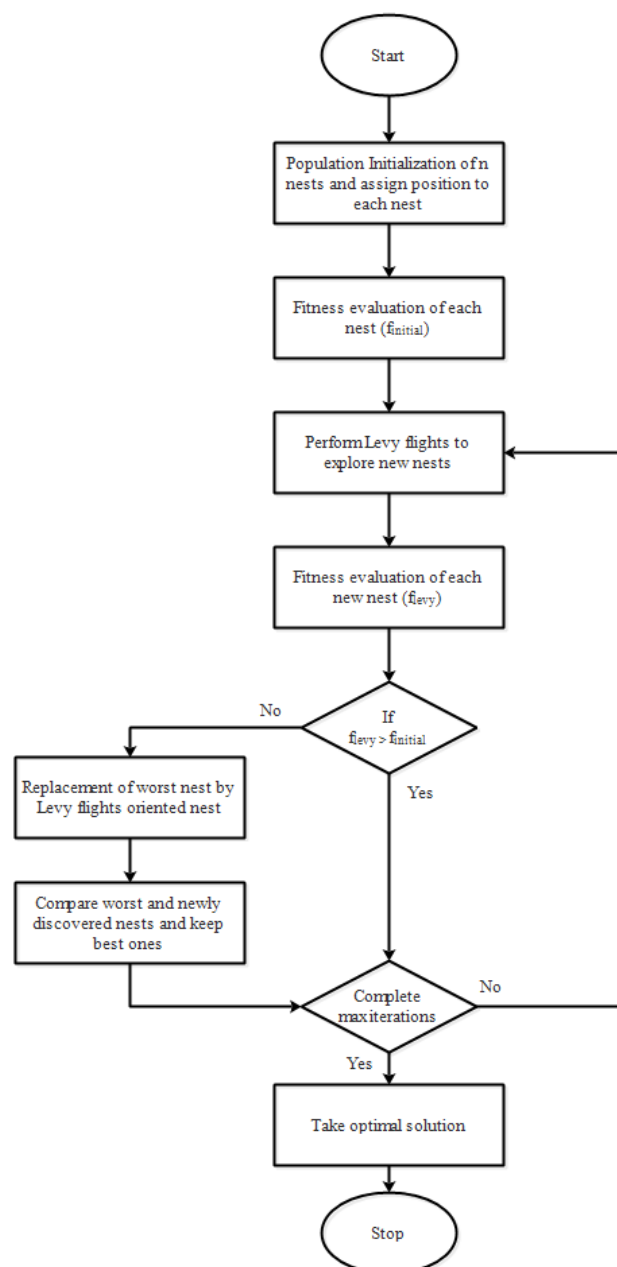


Figure 2. The description of cuckoo search algorithm.

Algorithm 1 Pseudocode: cuckoo search algorithm

```

Begin
   $F(\Phi), x = [\Phi_1, \Phi_2, \dots, \Phi_d]^T$ 
  Generate initial population
   $\Phi_i, (i = 1, 2, 3, \dots, n)$ 
  While ( $t < MaxGeneration$ ) or (stopping criterion)
    Cuckoo is picked randomly by level flights to analyze fitness
    Choose a nest randomly
  If ( $F_i > F_j$ )
    Old nest is abandoned and new nest will be built
    Keep the best solution
  Find the current best
End
  Post process results and visualizations
End

```

3.2. Particle Swarm Optimization

PSO is a nature inspired optimization technique based on the movement and intelligence of the swarm. In PSO, each particle continues to update its position under the previous experience and neighbours. A particle is composed of three vectors. The first is the x-vector, which records the current situation. The second one is the p-vector which records the location of the best solution in search space, and the third one is v-vector which contains the gradient for which particles will travel if undisturbed. The working of PSO can be explained in the following four steps as illustrated in Figure 3.

Step 1: Initialization: Random particles initialize the PSO algorithm, and each particle is a solution. Each particle searches for the optimum value by updating the generation. In each iteration, every particle is updated. After finding the best value, the particle updates its velocity and position. Particles can update their position by

$$x_i^{(t+1)} = x_i^{(t)} + v_i^{(t)} * t \quad (19)$$

Particle can update its velocity by the following equation

$$x_i^{(t+1)} = w * v_i^{(t)} + c_1 * v_1(xbest_i^t - x_i^t) + c_2 * r_2(gbest_i^t - x_i^t) \quad (20)$$

Step 2: Fitness investigation: The fitness size is analyzed for every particle. Choose the particle with the best fitness value.

Step 3: For each particle calculate velocity and position from Equations (1) and (2)

Step 4: Evaluate Fitness $f(x_i^t)$ Find current best

Step 5: Update $t = t + 1$

Step 6: Output gbest and $x_i(t)$

The process will be repeated until the condition is met.

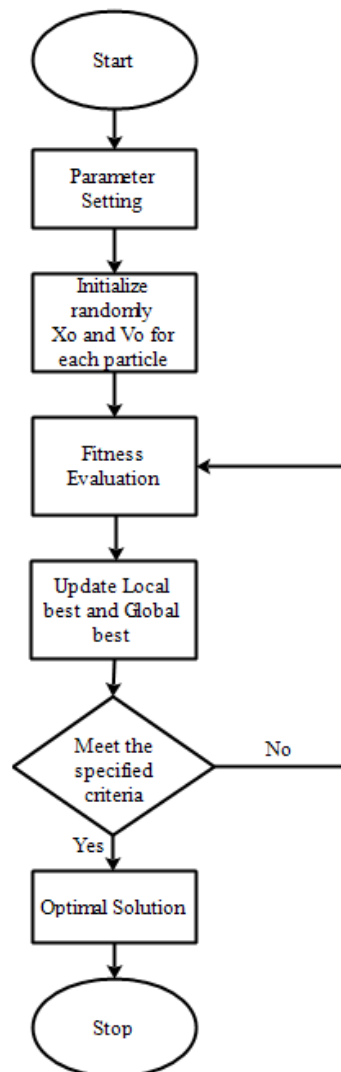


Figure 3. The explanation of particle swarm optimization in terms of a flow chart.

4. Results, Discussions and Achievements

In prior studies, uniform linear arrays and plenty of heuristic algorithms were used for DOA estimation. Still, in this work, we implemented a novel approach of the coprime array with a cuckoo search algorithm for DOA estimation. In this part of the paper, a series of experimental simulations are conducted to confirm the performance of the proposed scheme for DOA estimation. In our first experiment, we analyze the estimation accuracy of the proposed algorithm by comparing the results with PSO. After this analysis, the performance of root means square error (RMSE) by signal to noise ratio (SNR) and the number of snapshots is examined. Moreover, variation analysis, cumulative distribution function analysis and histogram analysis are also performed. The experimental analyses are categorized into three portions, six, nine and twelve sources estimations to validate our results and DOF.

4.1. Estimation Accuracy

Results for estimation accuracy of CS and PSO are obtained by setting different parameters as a signal-to-noise ratio, number of sources and their locations. The analysis is performed based on both algorithms' best, mean and worst estimations. In case of six sources, results for estimation accuracy of CS and PSO are quite well at 0 dB, -5 dB and -10 dB as shown in Tables 1–3.

Table 1. Calculation of accuracy for six targets at 0 dB SNR.

Actual Angles (Degrees)		$\Phi_1=20$	$\Phi_2=40$	$\Phi_3=60$	$\Phi_4=80$	$\Phi_5=100$	$\Phi_6=120$
CS	Best	19.957	40.002	59.826	79.889	99.897	120.003
	Mean	18.563	38.750	59.726	79.373	101.009	119.917
	Worst	8.322	35.5332	58.7853	79.738	99.970	120.058
PSO	Best	20.090	39.932	59.714	79.996	100.287	120.000
	Mean	16.361	37.489	59.579	79.983	100.113	119.697
	Worst	0.145	30.027	39.150	59.312	79.567	99.001

Table 2. Calculation of accuracy for six targets at -5 dB SNR.

Actual Angles (Degrees)		$\Phi_1=20$	$\Phi_2=40$	$\Phi_3=60$	$\Phi_4=80$	$\Phi_5=100$	$\Phi_6=120$
CS	Best	19.784	39.820	59.855	79.886	100.259	119.980
	Mean	21.610	40.151	59.092	79.256	101.344	120.111
	Worst	09.287	36.093	59.598	78.986	100.932	119.839
PSO	Best	19.961	40.075	59.884	79.839	99.788	120.000
	Mean	18.405	38.837	59.709	79.202	100.519	119.931
	Worst	0.000	32.679	39.566	58.822	79.662	98.929

Table 3. Calculation of accuracy for six targets at -10 dB SNR.

Actual Angles (Degrees)		$\Phi_1=20$	$\Phi_2=40$	$\Phi_3=60$	$\Phi_4=80$	$\Phi_5=100$	$\Phi_6=120$
CS	Best	20.470	40.140	59.923	79.942	100.017	120.297
	Mean	15.794	37.302	61.420	80.681	99.006	118.444
	Worst	33.509	58.204	77.819	101.635	121.967	180.000
PSO	Best	20.630	39.500	59.908	79.860	99.936	120.000
	Mean	16.630	36.413	59.679	78.153	101.692	120.000
	Worst	16.630	36.413	59.679	78.153	101.692	120.000

In the case of the nine sources estimation, the performance of CS is much better than PSO at 0 dB and -5 dB. At -10 dB performance of CS is slightly degraded but even then results are much better as compared to PSO as mentioned in Tables 4–6.

Table 4. Calculation of accuracy for nine targets at 0 dB SNR.

Actual Angles (Degrees)		$\Phi_1=20$	$\Phi_2=35$	$\Phi_3=50$	$\Phi_4=65$	$\Phi_5=80$	$\Phi_6=95$	$\Phi_7=110$	$\Phi_8=125$	$\Phi_9=140$
CS	Best	19.593	34.793	50.403	65.458	80.113	95.054	110.006	124.515	140.290
	Mean	21.243	33.810	51.328	64.016	76.648	91.598	106.852	123.380	140.346
	Worst	29.671	44.863	62.467	78.987	95.309	112.152	127.871	138.777	180.000
PSO	Best	21.756	34.090	50.015	61.225	74.220	88.506	100.388	109.193	120.000
	Mean	21.368	32.547	48.221	58.335	68.618	80.331	93.256	107.042	120.000
	Worst	03.442	33.559	34.329	52.492	59.308	74.175	90.715	106.549	120.000

Table 5. Calculation of accuracy for nine targets at -5 dB SNR.

Actual Angles (Degrees)		$\Phi_1=20$	$\Phi_2=35$	$\Phi_3=50$	$\Phi_4=65$	$\Phi_5=80$	$\Phi_6=95$	$\Phi_7=110$	$\Phi_8=125$	$\Phi_9=140$
CS	Best	19.644	36.090	50.107	64.055	79.008	94.836	110.112	125.026	140.428
	Mean	19.403	34.089	48.515	61.256	76.077	91.722	105.888	122.097	138.261
	Worst	34.872	47.166	62.034	79.183	95.973	112.682	127.446	137.827	179.951
PSO	Best	22.095	35.295	50.271	60.816	73.875	87.558	98.122	108.159	120.000
	Mean	21.727	34.366	47.335	57.730	70.796	80.923	93.077	106.002	120.000
	Worst	02.153	32.069	34.862	50.530	58.640	74.127	90.846	105.415	120.000

Table 6. Calculation of accuracy for nine targets at -10 dB SNR.

Actual Angles (Degrees)		$\Phi_1=20$	$\Phi_2=35$	$\Phi_3=50$	$\Phi_4=65$	$\Phi_5=80$	$\Phi_6=95$	$\Phi_7=110$	$\Phi_8=125$	$\Phi_9=140$
CS	Best	17.914	35.130	51.020	64.460	79.595	95.440	110.391	124.074	139.448
	Mean	13.768	32.605	47.946	64.958	79.856	98.667	113.959	130.077	140.819
	Worst	32.106	47.430	62.859	79.176	99.025	115.902	131.446	137.429	179.741
PSO	Best	25.352	34.606	53.414	65.818	76.683	91.433	103.044	109.174	120.000
	Mean	24.897	31.474	46.282	57.235	69.460	77.796	91.801	106.276	120.000
	Worst	01.602	32.134	35.065	49.745	60.489	69.987	80.391	96.584	111.233

In the case of the twelve sources estimation, CS again performed well, whereas PSO could not handle this scenario as well as CS. Performance of CS at 0 dB, -5 dB and -10 dB is remarkable in all three cases. Results obtained from CS and PSO are illustrated in Tables 7–9.

Table 7. Calculation of accuracy for twelve targets at 0 dB SNR.

Actual Angles (Degrees)		$\Phi_1=20$	$\Phi_2=30$	$\Phi_3=40$	$\Phi_4=50$	$\Phi_5=60$	$\Phi_6=70$	$\Phi_7=80$	$\Phi_8=90$	$\Phi_9=100$	$\Phi_{10}=110$	$\Phi_{11}=120$	$\Phi_{12}=130$
CS	Best	20.771	29.991	40.635	49.744	60.279	69.337	79.937	89.905	100.259	108.893	119.588	131.413
	Mean	15.644	33.214	36.495	49.199	58.992	68.778	78.185	88.490	99.042	107.952	118.438	130.534
	Worst	32.892	34.780	49.417	59.459	71.079	80.331	89.889	99.921	109.528	118.439	130.460	179.997
PSO	Best	25.423	25.724	43.204	51.689	63.631	71.924	82.989	90.470	100.336	107.281	120.000	120.000
	Mean	23.636	23.944	37.693	47.767	54.461	64.581	72.960	82.334	90.031	99.924	107.863	120.000
	Worst	21.932	30.708	31.234	49.225	49.640	63.914	70.749	80.705	88.585	98.879	107.166	120.000

Table 8. Calculation of accuracy for twelve targets at -5 dB SNR.

Actual Angles (Degrees)		$\Phi_1=20$	$\Phi_2=30$	$\Phi_3=40$	$\Phi_4=50$	$\Phi_5=60$	$\Phi_6=70$	$\Phi_7=80$	$\Phi_8=90$	$\Phi_9=100$	$\Phi_{10}=110$	$\Phi_{11}=120$	$\Phi_{12}=130$
CS	Best	20.609	30.658	40.470	49.065	58.658	69.505	79.987	90.209	99.895	108.988	120.244	130.064
	Mean	16.200	33.655	35.757	49.880	59.819	71.005	79.543	88.954	96.921	106.396	118.447	129.422
	Worst	33.631	36.751	51.618	60.733	71.977	80.107	91.166	100.355	110.272	121.987	130.929	180.000
PSO	Best	24.594	26.424	40.313	49.013	56.839	68.693	76.945	88.490	101.784	106.160	120.000	120.000
	Mean	19.786	30.707	37.353	51.786	52.633	66.785	72.0238	83.242	88.560	98.188	105.903	120.000
	Worst	18.306	29.093	29.594	46.470	49.143	61.943	69.262	78.375	87.403	96.631	106.210	120.000

Table 9. Calculation of accuracy for twelve targets at -10 dB SNR.

Actual Angles (Degrees)		$\Phi_1=20$	$\Phi_2=30$	$\Phi_3=40$	$\Phi_4=50$	$\Phi_5=60$	$\Phi_6=70$	$\Phi_7=80$	$\Phi_8=90$	$\Phi_9=100$	$\Phi_{10}=110$	$\Phi_{11}=120$	$\Phi_{12}=130$
CS	Best	19.231	30.410	39.738	50.089	59.972	68.568	78.721	89.754	101.099	110.242	118.923	128.847
	Mean	13.739	32.169	36.198	46.861	59.284	69.950	80.950	93.324	103.538	113.336	121.217	132.087
	Worst	32.608	34.556	46.973	59.788	64.350	78.185	95.780	106.395	114.413	122.340	132.117	180.000
PSO	Best	25.788	26.402	41.916	51.693	60.857	68.785	79.025	90.077	101.744	108.859	119.960	120.000
	Mean	20.911	30.796	36.900	49.856	56.640	71.017	71.499	84.186	91.056	101.661	106.794	120.000
	Worst	5.759	28.905	29.014	42.225	47.788	59.724	65.001	76.072	87.495	97.088	108.557	120.000

4.2. Overview of Robustness against Noise

Robustness against noise is considered a powerful tool for evaluating the outcomes of parameters estimation algorithms in radar array signal processing. In this analysis, the value of RMSE is monitored at different SNR levels. Therefore, RMSE is called a performance indicator in this analysis. In Figure 4, CS shows much robustness against noise than PSO. When SNR is increased from -15 dB to -5 dB, the value of RMSE decreases abruptly in the case of six sources. In the scenario of nine sources estimation, CS performs much better than PSO, as shown in Figure 5. Similarly, in the case of twelve sources, again, CS provides better results than PSO, as illustrated in Figure 6. In all of the instances, CS performs much better than PSO for the direction of arrival estimation.

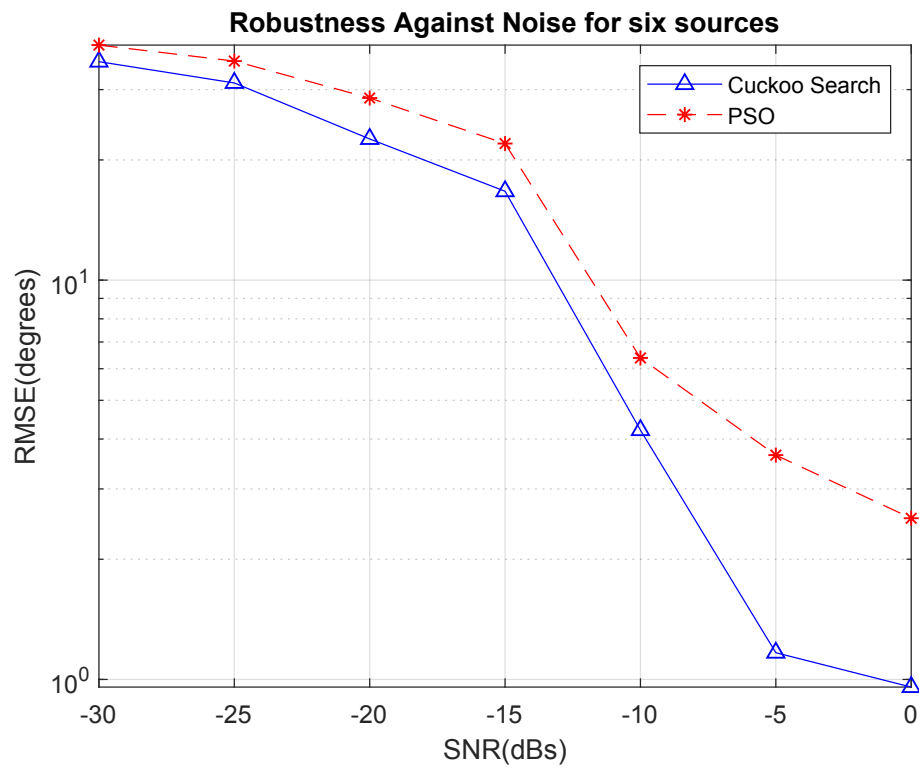


Figure 4. Estimation of robustness using six sources.

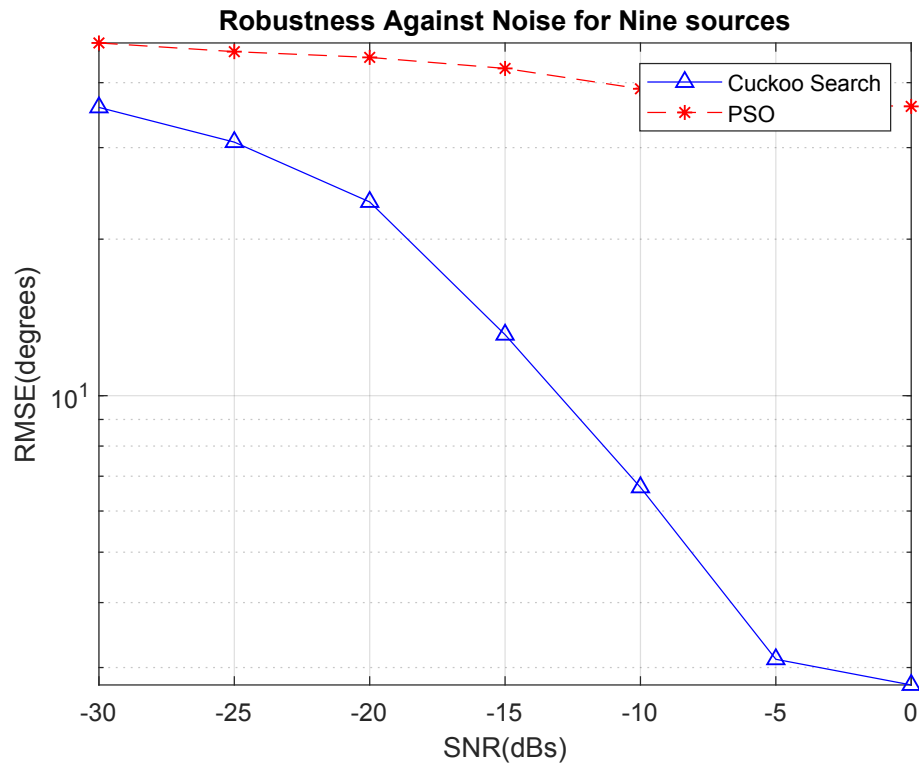


Figure 5. Robustness against noise for nine sources.

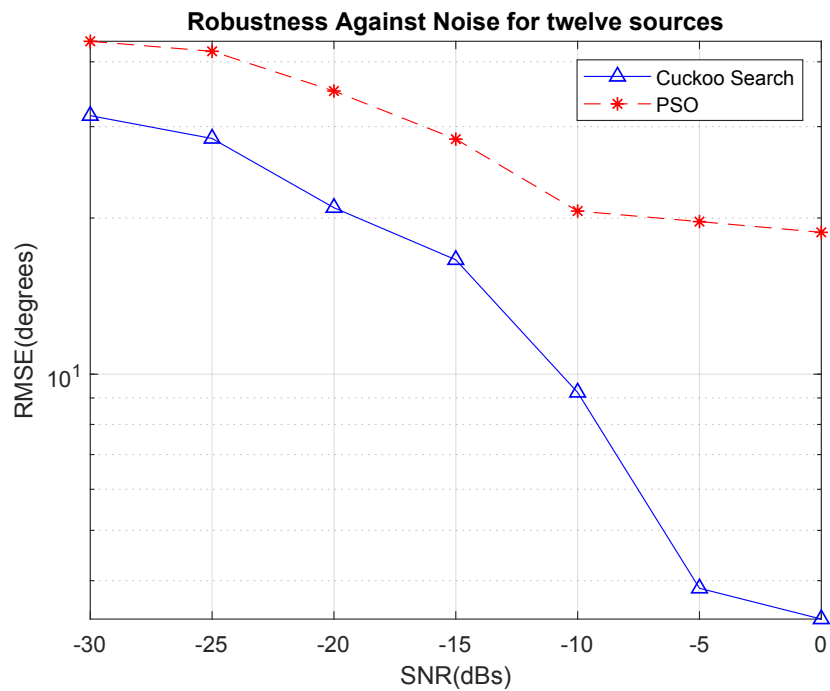


Figure 6. Robustness against noise for twelve sources.

4.3. RMSE Analysis against Multiple Snapshots

In this analysis, we investigate the value of RMSE against multiple snapshots. Therefore, this analysis is also known as robustness against snapshots. In Figure 7, we examine that value of RMSE of CS is decreasing as the number of snapshots increases as compared to PSO. In the region of 0 to 100 snapshots, RMSE is falling off rapidly for both optimization schemes, and the overall performance of CS is better than PSO. In the scenario of nine and twelve targets estimation, the version of CS is better than PSO. Therefore, the required degree of freedom is achieved using CS, as shown in Figures 8 and 9.

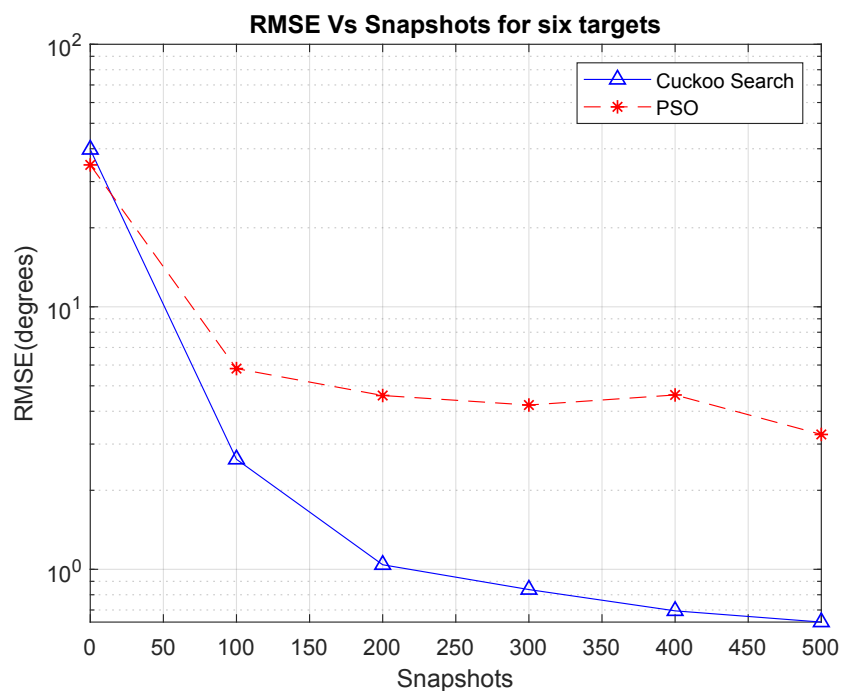


Figure 7. Estimation of robustness using six sources in terms of snapshots.

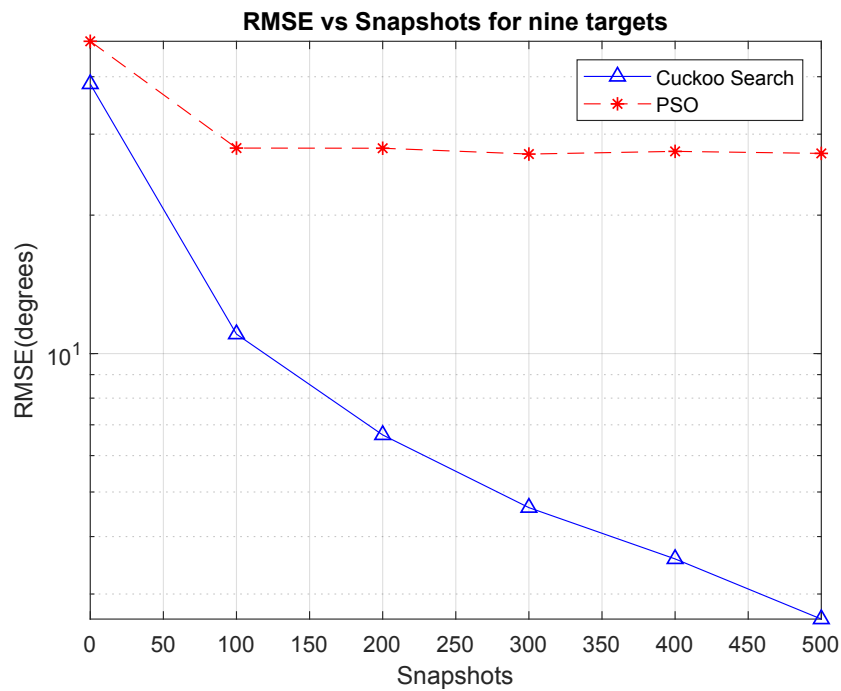


Figure 8. Estimation of robustness using nine sources in terms of snapshots.

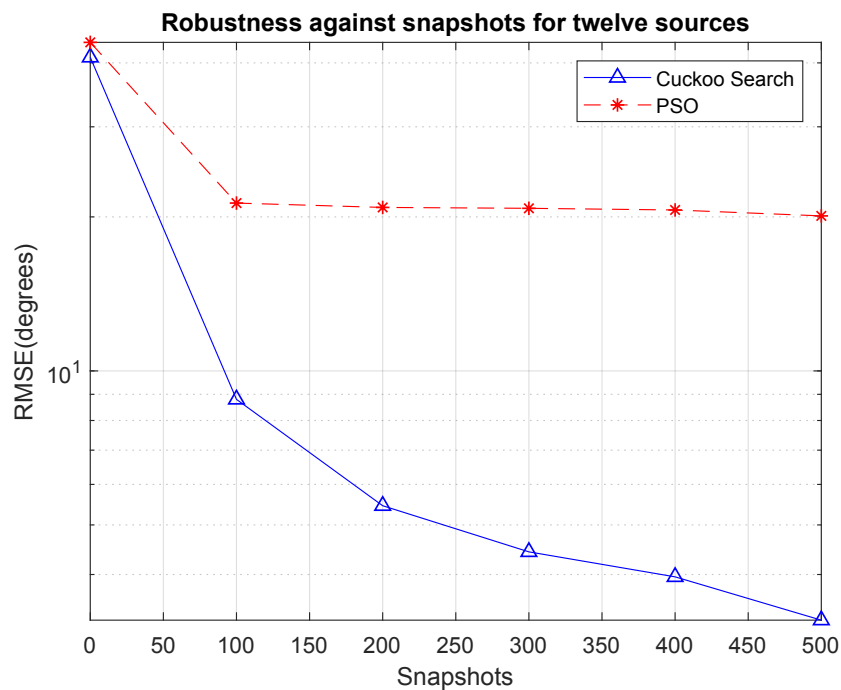


Figure 9. Estimation of robustness using twelve sources in terms of snapshots.

4.4. Variation Analysis of RMSE

Variation analysis of RMSE is one of the popular tools to express the distribution of error concerning Q_1, Q_2, Q_3 min and max values of given data. These values are distinguished using outlier, where the performance of estimation algorithm can be easily identified of used parameters. The performance of proposed CS and PSO are compared in Figure 10 for maximum RMSE of FPA using 40, 55 and 60 at 0 dB, -5 dB and -10 dB, respectively. The result elaborates the outcomes of FPA against the current PSO system.

As for nine targets, the RMSE of FPA has less expansion than PSO at 0, -5 and 10 dB as mentioned in Figure 11. Similar performance of FPA as compared to PSO can be seen in Figure 12 at 0, -5 and -10 dB.

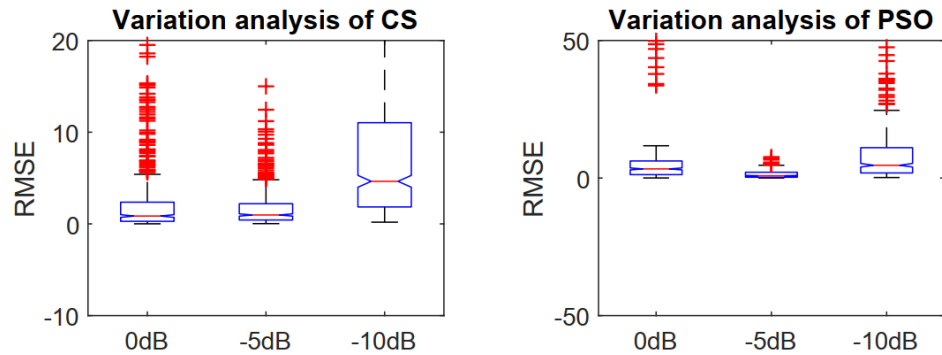


Figure 10. Variation analysis of CS and PSO by estimating six sources.

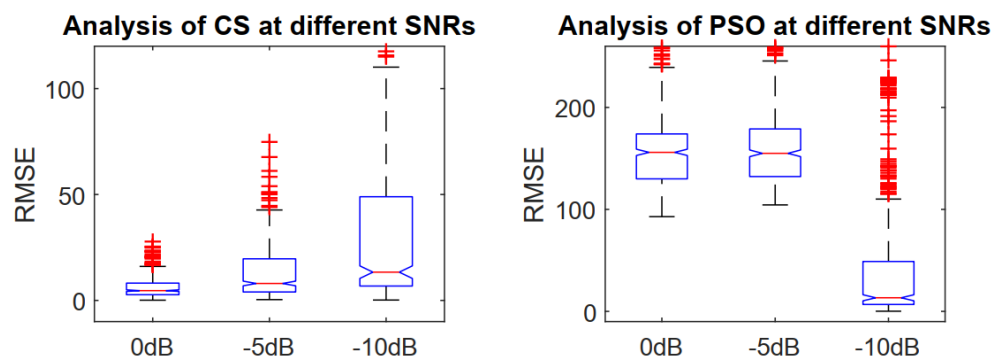


Figure 11. Variation analysis of CS and PSO by estimating nine sources.

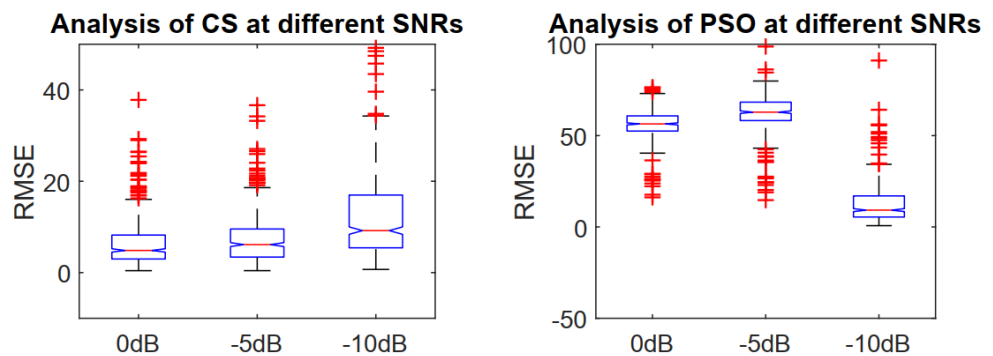


Figure 12. Variation analysis of CS and PSO by estimating twelve sources.

4.5. Cumulative Distribution Function of RMSE

The cumulative distribution function belongs to the family of non-decreasing functions. This function shows the steadiness and failure of the optimization techniques based on Monte Carlo simulation runs. In Figure 13, at 0 dB, RMSE occurred after 75% runs in the case of CS optimization, and RMSE occurred at 30% of Monte Carlo simulation runs of PSO optimization. At -5 dB, RMSE occurred after 50% Monte Carlo simulation runs in

both algorithms. RMSE rises in CS algorithm after 60% of Monte Carlo simulation runs, and in PSO algorithm, it raised after 40% of Monte Carlo simulation runs. At -10 dB, RMSE occurred at 40% of Monte Carlo simulation runs, but an increase in RMSE is more rapid in PSO than CS. So the overall performance of CS is strongly preferable concerning PSO in the case of six sources estimation.

In the case of nine and twelve sources estimation, the performance of CS is significantly better than PSO, as shown in Figures 14 and 15. We have successfully achieved the maximum DOF of coprime arrays up to $O(MN)$ by estimating twelve sources through the CS algorithm.

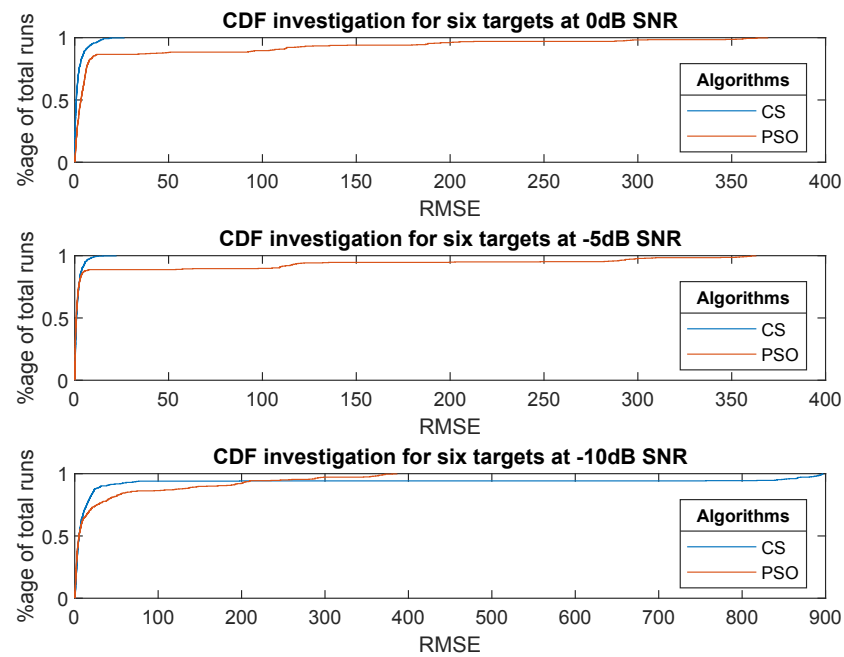


Figure 13. RMSE investigation in terms of CDF using six targets for various values of SNR.

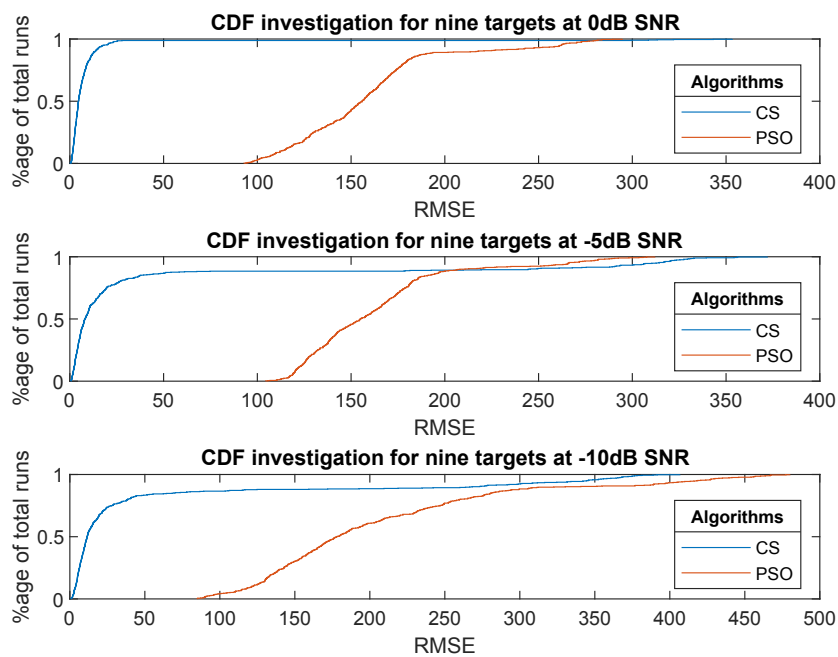


Figure 14. RMSE investigation in terms of CDF using nine targets for various values of SNR.

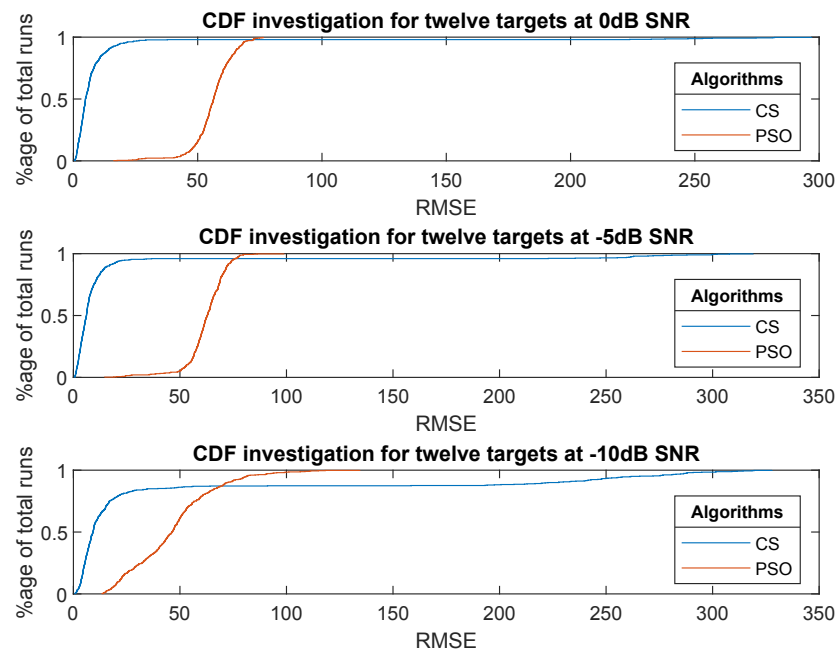


Figure 15. RMSE investigation in terms of CDF using twelve targets for various values of SNR.

4.6. Histogram Analysis of RMSE

Histogram analysis shows how much error occurred against the different Monte Carlo simulation runs. By this analysis, we evaluate the performance of optimization schemes. In histogram analysis, bars are in the form of continuous grouping. In the case of six sources estimation, RMSE of CS and PSO is very good at 0 dB, -5 dB and -10 dB SNR over the 500 iterations. Figure 16 explored the analysis for nine targets in terms of RMSE and compared the outcomes among proposed CS and PSO, where the performance of CS is more efficient than PSO. Furthermore, the spread of RMSE at 0, -5 and 10 dB is analyzed for PSO using 500 iterations as discussed in Figures 17 and 18.

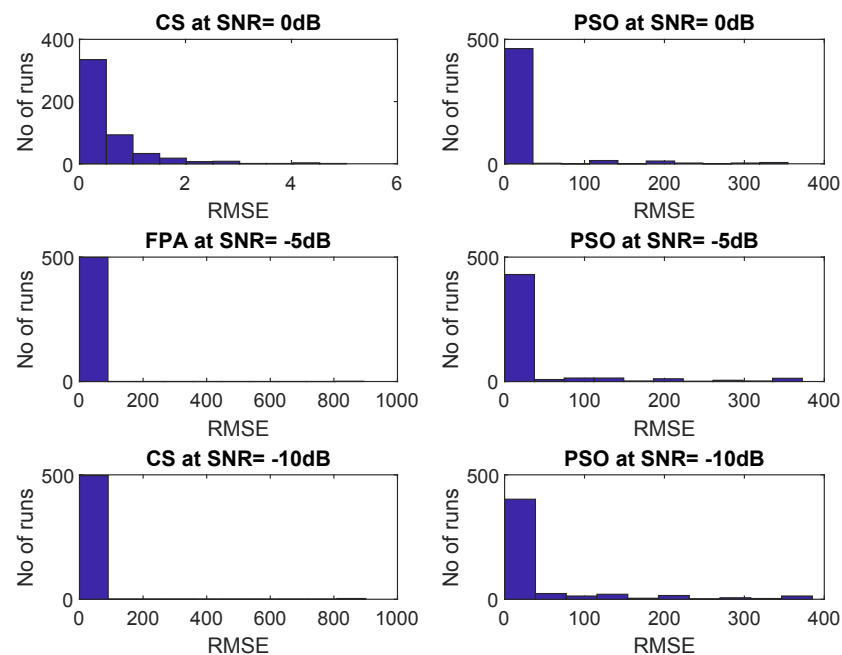


Figure 16. Correlation of proposed CS and PSO models based on RMSE using six targets.

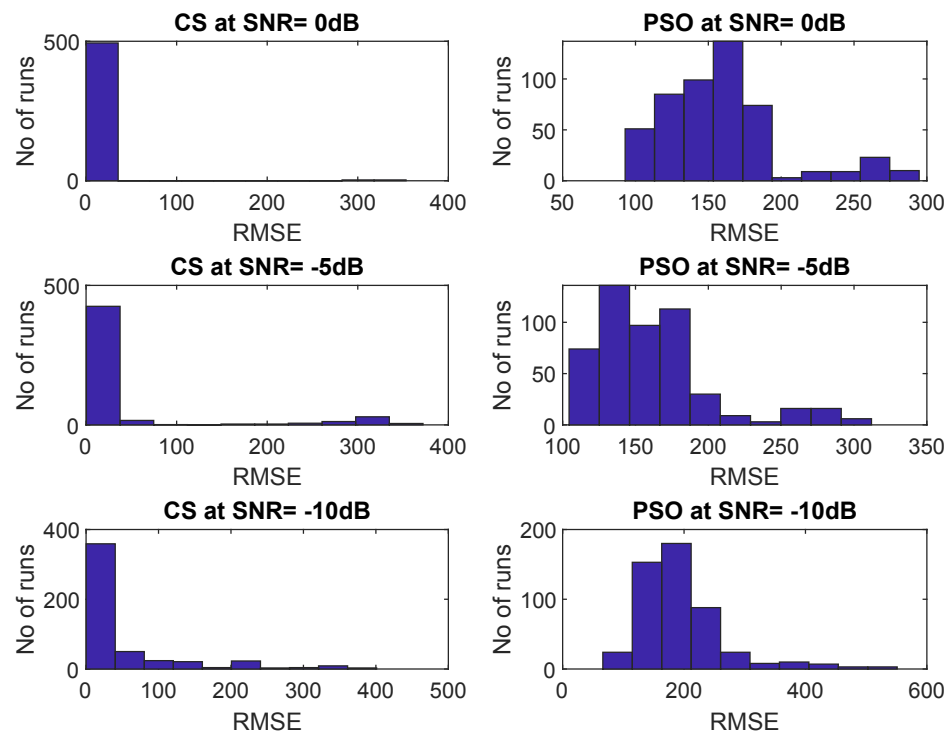


Figure 17. Correlation of proposed CS and PSO models based on RMSE using nine targets.

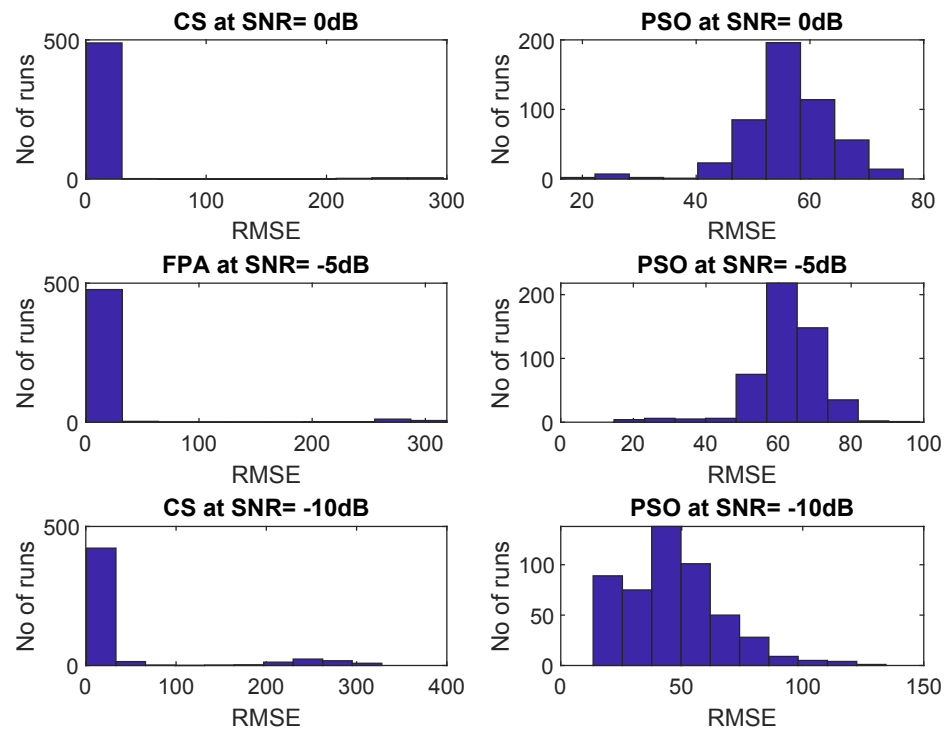


Figure 18. Correlation of proposed CS and PSO models based on RMSE using twelve targets.

5. Conclusions

This paper estimates the DOA of electromagnetic waves for far-field sources by implementing coprime arrays through a cuckoo search algorithm. We have achieved maximum freedom in a low SNR environment using metaheuristic algorithms while the performance of deterministic algorithms is degraded at a low SNR regime. Nevertheless, cuckoo search provides better resolution and higher DOF at low SNR. In the future, we can also estimate

the frequency, amplitude and other parameters of the electromagnetic wave as per our requirement by using this methodology.

Author Contributions: Conceptualization, K.H., F.A., W.K., M.S.Q. and A.A.; methodology, M.A. (Muhammad Asif), Y.S.A., F.F.A.-H., M.A. (Mohammad Alibakhshikenari), and M.D.; software, K.H., F.A. and M.S.M.; validation, F.F.A.-H., M.S.M., M.A. (Mohammad Alibakhshikenari) and M.D.; formal analysis, K.H.; investigation, M.A. (Mohammad Alibakhshikenari), M.D.; resources, M.A. (Muhammad Asif); data curation, Y.S.A., F.F.A.-H.; writing—original draft preparation, K.H., F.A.; writing—review and editing, F.F.A.-H., A.A., M.A. (Muhammad Asif), F.A., M.S.M. M.A. (Mohammad Alibakhshikenari) and M.D.; visualization, K.H., F.A., M.A. (Mohammad Alibakhshikenari) and M.D.; supervision, K.H., F.A., M.A. (Mohammad Alibakhshikenari), M.D.; project administration, F.A., M.A. (Muhammad Asif), M.A. (Mohammad Alibakhshikenari) and M.D.; funding acquisition, M.A. (Mohammad Alibakhshikenari) and M.D. All authors have read and agreed to the published version of the manuscript.

Funding: This project has received funding from Universidad Carlos III de Madrid and the European Union’s Horizon 2020 research and innovation programme under the Marie Skłodowska-Curie Grant 801538.

Data Availability Statement: All data and research finding are included withing the manuscript.

Acknowledgments: The authors sincerely appreciate the supports from Universidad Carlos III de Madrid and the European Union’s Horizon 2020 research and innovation programme under the Marie Skłodowska-Curie Grant 801538. The authors express their gratitude to Princess Nourah bint Abdulrahman University Researchers Supporting Project (Grant No. PNURSP2022R55), Princess Nourah bint Abdulrahman University, Riyadh, Saudi Arabia.

Conflicts of Interest: The authors declare no conflict of interest.

References

1. Wu, J.; Bao, C. Multiple target DOA estimation with single snapshot in sonar array. Eleventh International Conference on Signal Processing Systems. *Int. Soc. Opt. Photonics* **2019**, *11384*, 113840L.
2. Wang, J.; Xu, H.; Leus, G.J.; Vandenbosch, G.A. Experimental assessment of the coarray concept for DoA estimation in wireless communications. *IEEE Trans. Antennas Propag.* **2018**, *66*, 3064–3075. [[CrossRef](#)]
3. Huang, L.; Lu, Z.; Xiao, Z.; Ren, C.; Song, J.; Li, B. Suppression of Jammer Multipath in GNSS Antenna Array Receiver. *Remote Sens.* **2022**, *14*, 350. [[CrossRef](#)]
4. Lehtonen, O. Medical Ultrasound Imaging Using Sparse Arrays. Master’s Thesis, Aalto Universit, Espoo, Finland, 2021.
5. Zhou, C.; Shi, Z.; Gu, Y.; Shen, X. DECOM: DOA estimation with combined MUSIC for coprime array. In Proceedings of the 2013 International Conference on Wireless Communications and Signal Processing, Hangzhou, China, 24–26 October 2013; pp. 1–5.
6. Guo, M.; Zhang, Y.D.; Chen, T. DOA estimation using compressed sparse array. *IEEE Trans. Signal Process.* **2018**, *66*, 4133–4146. [[CrossRef](#)]
7. Qin, G.; Amin, M.G.; Zhang, Y.D. DOA estimation exploiting sparse array motions. *IEEE Trans. Signal Process.* **2019**, *67*, 3013–3027. [[CrossRef](#)]
8. Wajid, M.; Kumar, B.; Goel, A.; Kumar, A.; Bahl, R. Direction of arrival estimation with uniform linear array based on recurrent neural network. In Proceedings of the 2019 5th International Conference on Signal Processing, Computing and Control (ISPCC), Solan, India 10–12 October 2019; pp. 361–365.
9. Wu, H.; Shen, Q.; Liu, W.; Cui, W. Underdetermined low-complexity wideband DOA estimation with uniform linear arrays. In Proceedings of the 2020 IEEE 11th Sensor Array and Multichannel Signal Processing Workshop (SAM), Hangzhou, China, 8–11 June 2020; pp. 1–5.
10. Hammed, K.; Ghauri, S.A.; Qamar, M.S. Biological inspired stochastic optimization technique (PSO) for DOA and amplitude estimation of antenna arrays signal processing in RADAR communication system. *J. Sens.* **2016**, *2016*, 9871826. [[CrossRef](#)]
11. Papageorgiou, G.K.; Sellathurai, M. Fast direction-of-arrival estimation of multiple targets using deep learning and sparse arrays. In Proceedings of the ICASSP 2020-2020 IEEE International Conference on Acoustics, Speech and Signal Processing (ICASSP), Barcelona, Spain, 4–8 May 2020; pp. 4632–4636.
12. Hameed, K.; Tu, S.; Ahmed, N.; Khan, W.; Armghan, A.; Alenezi, F.; Alnaim, N.; Qamar, M.S.; Basit, A.; Ali, F. DOA Estimation in Low SNR Environment through Coprime Antenna Arrays: An Innovative Approach by Applying Flower Pollination Algorithm. *Appl. Sci.* **2021**, *11*, 7985. [[CrossRef](#)]
13. Geng, W.; Changxiao, C.; Yi, H.; Mingyue, F.; Jiang, Y.; Zhao, R. 2-D DOA Estimation Based on Rectangular Generalized Minimum Redundancy Array via Partial Grid Covariance Vector Sparse Reconstruction. In Proceedings of the 2021 6th International Conference on Intelligent Computing and Signal Processing (ICSP), Xi’an, China, 9–11 April 2021; pp. 859–864.

14. Wang, G.; He, M.; Yu, C.; Han, J.; Chen, C. Fast Underdetermined DOA Estimation Based on Generalized MRA via Original Covariance Vector Sparse Reconstruction. *IEEE Access* **2021**, *9*, 66805–66815. [[CrossRef](#)]
15. Zheng, Z.; Yang, C.; Wang, W.Q.; So, H.C. Robust DOA estimation against mutual coupling with nested array. *IEEE Signal Process. Lett.* **2020**, *27*, 1360–1364. [[CrossRef](#)]
16. Zhou, C.; Gu, Y.; Shi, Z.; Haardt, M. Direction-of-arrival estimation for coprime arrays via coarray correlation reconstruction: A one-bit perspective. In Proceedings of the 2020 IEEE 11th Sensor Array and Multichannel Signal Processing Workshop (SAM), Hangzhou, China, 8–11 June 2020; pp. 1–4.
17. Moffet, A. Minimum-redundancy linear arrays. *IEEE Trans. Antennas Propag.* **1968**, *16*, 172–175. [[CrossRef](#)]
18. Pal, P.; Vaidyanathan, P.P. Nested arrays: A novel approach to array processing with enhanced degrees of freedom. *IEEE Trans. Signal Process.* **2010**, *58*, 4167–4181. [[CrossRef](#)]
19. Zhou, C.; Zhou, J. Direction-of-arrival estimation with coarray ESPRIT for coprime array. *Sensors* **2017**, *17*, 1779. [[CrossRef](#)] [[PubMed](#)]
20. Qamar, M.S.; Tu, S.; Ali, F.; Armghan, A.; Munir, M.F.; Alenezi, F.; Muhammad, F.; Ali, A.; Alnaim, N. Improvement of Traveling Salesman Problem Solution Using Hybrid Algorithm Based on Best-Worst Ant System and Particle Swarm Optimization. *Appl. Sci.* **2021**, *11*, 4780. [[CrossRef](#)]
21. Liu, A.; Yang, D.; Shi, S.; Zhu, Z.; Li, Y. Augmented subspace MUSIC method for DOA estimation using acoustic vector sensor array. *IET Radar Sonar Navig.* **2019**, *13*, 969–975. [[CrossRef](#)]
22. Vikas, B.; Vakula, D. Performance comparison of MUSIC and ESPRIT algorithms in presence of coherent signals for DoA estimation. In Proceedings of the 2017 International Conference of Electronics, Communication and Aerospace Technology (ICECA), Coimbatore, India, 20–22 April 2017; Volume 2, pp. 403–405.
23. Zhang, D.; Zhang, Y.; Zheng, G.; Feng, C.; Tang, J. Improved DOA estimation algorithm for co-prime linear arrays using root-MUSIC algorithm. *Electron. Lett.* **2017**, *53*, 1277–1279. [[CrossRef](#)]
24. Yao, B.; Zhang, W.; Wu, Q. Weighted subspace fitting for two-dimension DOA estimation in massive MIMO systems. *IEEE Access* **2017**, *5*, 14020–14027. [[CrossRef](#)]
25. Ahmed, N.; Wang, H.; Raja, M.A.Z.; Ali, W.; Zaman, F.; Khan, W.U.; He, Y. Performance analysis of efficient computing techniques for direction of arrival estimation of underwater multi targets. *IEEE Access* **2021**, *9*, 33284–33298. [[CrossRef](#)]
26. Chang, J.C. DOA Estimation for local scattered cdma signals by particle swarm optimization. *Sensors* **2012**, *12*, 3228–3242. [[CrossRef](#)]
27. Sheikh, Y.A.; Zaman, F.; Qureshi, I.; Atique-ur Rehman, M. Amplitude and direction of arrival estimation using differential evolution. In Proceedings of the 2012 International Conference on Emerging Technologies, Islamabad, Pakistan, 8–9 October 2012; pp. 1–4.
28. Jia, W.; Liu, S. Application of simulated annealing genetic algorithm in DOA estimation technique. *Comput. Eng. Appl.* **2014**, *50*, 266–270.
29. Mao, L.; Zhang, Q.; Huang, J.; Han, J. Maximum likelihood direction of arrival estimator based on modified ant colony optimization. In Proceedings of the 2013 IEEE International Conference of IEEE Region 10 (TENCON 2013), Xi'an, China, 22–25 October 2013; pp. 1–4.
30. Parsa, S.A.; Zadeh, A.E.; Kazemitabar, S.J. A Novel Modified Artificial Bee Colony for DOA Estimation. *Int. J. Sens. Wirel. Commun. Control* **2021**, *11*, 96–106. [[CrossRef](#)]
31. Akbar, S.; Raja, M.A.Z.; Chaudhary, N.I.; Zaman, F.; Alquhayz, H. Flower Pollination Heuristics for Parameter Estimation of Electromagnetic Plane Waves. *CMC Comput. Mater. Contin.* **2021**, *68*, 2529–2543. [[CrossRef](#)]
32. Gandomi, A.H.; Yang, X.S.; Alavi, A.H. Cuckoo search algorithm: A metaheuristic approach to solve structural optimization problems. *Eng. Comput.* **2013**, *29*, 17–35. [[CrossRef](#)]